Low Complexity CFO Compensation in Uplink OFDMA Systems with Receiver Windowing

Arman Farhang*, Nicola Marchetti*, Linda E. Doyle* and Behrouz Farhang-Boroujeny†
*CTVR / CONNECT, The Telecommunications Research Centre, Trinity College Dublin, Ireland,
†ECE Department, University of Utah, USA.
Email: {farhanga, marchetn, ledoyle}@tcd.ie, farhang@ece.utah.edu

***Abstract*—Orthogonal frequency division multiple access (OFDMA) systems in the uplink suffer from multiple access interference (MAI) due to their high sensitivity to frequency misalignments between different users. In this paper, we propose the application of time domain receiver windowing methods to confine the leakage caused by multiple carrier frequency offsets (CFOs) to a few neighbouring subcarriers with almost no additional computational burden. The CFO effects can be translated into a linear system of equations with a coefficient matrix that is called *interference matrix*. As a result of receiver windowing, we can approximate the interference matrix with a quasi-banded one by neglecting its small elements outside a certain bandwidth. This allows us to propose a class of low complexity CFO compensation techniques. These techniques are applicable to the generalized subcarrier allocation scheme (G-CAS). The complexity reduction in the proposed solutions is substantial when compared to the existing ones in the literature. It is worth mentioning that this substantial complexity reduction is achieved in expense of some bandwidth efficiency loss. Hence, there exists a tradeoff between bandwidth efficiency and complexity. Solutions based on both zero forcing (ZF) and minimum mean squared error (MMSE) criteria are proposed and compared. Simulation results demonstrating the effectiveness of the proposed algorithms in approaching the optimal performance are also presented.**

I. Introduction

THIS paper focuses on low complexity carrier frequency offset (CFO) compensation methods for the uplink of orthogonal frequency division multiple access (OFDMA) systems. OFDMA systems are very sensitive to synchronization errors especially in the uplink. Imperfect synchronization breaks the orthogonality among the subcarriers and creates a great amount of multiple access interference as well as self-user interference [2]. As is prescribed in [3], the choice of long enough cyclic prefix (CP) will help the system to avoid the multiple access interference (MAI) caused by the timing misalignment of the users with respect to each other. Therefore, the timing mismatch between the users will be absorbed into their channel impulse responses and can be compensated at the channel equalization stage [3]. Due to the local oscillator misalignments and Doppler frequency shifts of different users in the uplink, multiple CFOs will appear in the received signal at the base station (BS). This results in a great amount of inter-carrier interference (ICI) and hence MAI. To compensate for the interference caused by the CFOs, first of all, an appropriate signal processing method is required to estimate the CFOs. Multiple CFOs estimation can be performed by application of one of the proposed algorithms in the literature [3]–[8]. Once the CFOs are estimated, a compensation technique is needed to remove the self-user and multiuser ICI, which we name respectively, ICI and MAI.

In OFDMA systems, there are a number of ways that carriers can be allocated to the users, namely: block carrier allocation, interleaved carrier allocation, block-interleaved carrier allocation and generalized carrier allocation schemes (G-CAS) [3]. Hence, if a compensation method is applicable to the G-CAS case, then all the options are covered. The focus of this paper is on the development of low complexity CFO compensation methods for the uplink of OFDMA systems with G-CAS.

The removal of self-user interference and MAI is a well tackled problem and solutions have been proposed in the literature, [9]–[17]. Some researchers have concentrated on interference cancellation methods. In [9] and [16], the authors propose interference cancellation techniques to remove ICI and MAI using tentatively detected data symbols of different users in an iterative manner. This study is extended by Chen et al. in [17] where they suggest a joint minimum mean square error frequency domain equalization (MMSE-FDE) and CFO compensation technique with interference cancellation. Ahmed and Zhang, [10], suggest a method of preconditioning the received signal vector, before applying the DFT, in order to limit the interfering subcarriers to a few adjacent ones. This preconditioning reduces the complexity of successive interference cancellation. This method was originally introduced by Schniter, [18], in the context of single user OFDM systems with time varying channels. The drawback of the interference cancellation solutions is that their performance degrades as CFOs increase [9], [10], [16]. Besides their high computational complexity, such methods may suffer from the error propagation problem, since wrong decisions may be fed back for cancellation.

The second class of CFO compensation techniques, which is of more interest in this paper, translates the effect of the CFOs into a linear system of equations with a coefficient matrix which is called *interference matrix*. In these techniques, the output of the DFT block at the BS is modeled as multiplication of the interference matrix to a composite data vector which contains the data of all the users, affected by their wireless channels. Solving this system of equations eliminates the MAI as well as self-user interference completely. However, it needs the inversion of an interference matrix, i.e., a square

A minor part of this paper is presented in IEEE WCNC 2014 [1].

matrix of size equal to the total number of subcarriers which can be as large as a few thousands in practical systems. Obviously, this makes the solution prohibitively complex. Thus, low complexity solutions have to be sought. Such a solution for the systems with interleaved subcarrier allocation is proposed by Hsu and Wu [13]. In a more recent work, [12], the authors suggested solutions that take advantage of the block circulant structure of the interference matrix in systems with interleaved and block-interleaved subcarrier allocation to further reduce the computational cost. Another relevant work is that of Cao et al., [11], where the authors approximated the interference matrix by a banded matrix, simply by assuming that the elements of the matrix outside a bandwidth D (a design parameter) are equal to zero. It is then noted that this approximation of the interference matrix can be used to find the desired solution with a low computational complexity that is in the order of ND^2, where N is the total number of subcarriers. However, as mentioned in [14], this approximation results in a significant performance loss, hence may not be a viable solution in practice. Huang et al., [19], have proposed an iterative ICI cancellation technique based on the Neumann power series expansion. However, it has been noted that this method has certain limitations in terms of carrier allocation. In [14], Lee et al. introduced an MMSE compensation technique using conjugate gradient algorithm. This method has a much lower complexity compared to its predecessors and is also applicable to the systems that use the generalized carrier allocation scheme, while maintaining the optimal performance. It is worth mentioning that CG algorithm is a fast implementation of MMSE solution and provides the same result as the direct MMSE solution [14]. Thus, we choose conjugate gradient (CG) algorithm as a benchmark.

The challenge for this paper, therefore, is to design a CFO compensation technique which has the following traits - (1) it is suitable for a wide range of CFOs (2) it has a lower computational complexity than our benchmark (CG algorithm) and (3) it is applicable to G-CAS.

Our solution combines a number of different ideas and concepts. It is based on time domain approaches. It draws on the fact that through time domain windowing, the interference matrix can be well approximated with a quasi-banded one. Hence, a very simple time domain processing introduces a means of confining the interference matrix and leads to low complexity CFO compensation techniques. However, it goes much further in the reduction of complexity through the introduction of a zero forcing (ZF) technique based on LU-factorization. As the paper will show, this results in a technique that can work with all values of CFOs within the range of $\pm 50\%$ of the subcarrier spacing, is over an order of magnitude lower in complexity than our benchmark CG algorithm, and can be used in G-CAS scenarios. Furthermore, we show even more complexity reduction (two orders of magnitude) still is possible in cases where CFOs are less than 25% of the subcarrier spacing through our proposed ZF technique based on Neumann series.

The paper also carries out some additional analysis. As MMSE approaches are generally seen as superior techniques over ZF approaches, we also extend our algorithms to include the MMSE case. However, it turns out that there is a negligible difference between the MMSE and the ZF solutions in the case of interest in this paper.

The significant reduction in complexity that our algorithms provide comes at the expense of some moderate loss in bandwidth efficiency which is due to the need for longer cyclic extentions in OFDM signal required for time domain windowing operations. Hence, there is a tradeoff between computational complexity and bandwidth efficiency. Our solutions are attractive to some emerging applications like *machine type communications* and *Internet of Things* (IoT) where there is a large number of users in a cell with different CFOs. In these applications, our proposed solutions can provide the optimal performance with an affordable computational complexity and as these systems do not need to have very high bit rates, the bandwidth efficiency loss due to windowing operation may not be critical, [20].

The rest of this paper is organized as follows. To lay down the problem that we plan to solve in the rest of the paper, a summary of the CFO formulation, in the uplink of OFDMA systems, is presented in Section II. This formulation shows that multiuser compensation can be achieved by solving a linear system of equations. The coefficient matrix of this system of equations is known as the interference matrix. Section III introduces the time domain windowing at the receiver, [21], as a means of reducing the interference matrix to a quasi-banded one. This paves the way for the introduction of a novel class of ZF and MMSE CFO compensation techniques that are presented in Section IV and Section V, respectively. A new version of the CG algorithm, for the case of interest in this paper, is also presented. A system complexity analysis that compares the proposed methods with their counterpart from literature having the lowest complexity, [14], is presented in Section VI. Numerical results are discussed in Section VII. Finally, the conclusions of the paper are drawn in Section VIII.

Notations: Matrices, vectors and scalar quantities are denoted by boldface uppercase, boldface lowercase and normal letters, respectively. $[\mathbf{A}]_{m,n}$ represents the element in the m^{th} row and n^{th} column of matrix $\mathbf{A}$, $\mathbf{A}^{-1}$ signifies the inverse of $\mathbf{A}$, $\mathbf{I}_M$ is the identity matrix of size M and $\mathbf{0}_{m\times n}$ is the zero matrix of size m by n. $\sigma(\mathbf{A})$ indicates the set of distinct eigenvalues of the matrix $\mathbf{A}$ and is called the *spectrum* of $\mathbf{A}$. $\mathrm{Rank}(\mathbf{A})$, $\mathrm{Range}(\mathbf{A})$, $\mathrm{Null}(\mathbf{A})$ and $\mathrm{Dim}(\mathbf{A})$ indicate rank, range, nullspace and dimension of $\mathbf{A}$, respectively [22]. The superscripts $(\cdot)^{\mathrm{T}}$ and $(\cdot)^{\mathrm{H}}$ indicate transpose and conjugate transpose of a matrix, respectively. Finally, $\mathrm{diag}(\mathbf{x})$, $*$ and $|\cdot|$ represent a diagonal matrix with diagonal elements of the vector $\mathbf{x}$, linear convolution and absolute value, respectively.

II. System Model

The uplink of an OFDMA system with K users and one base station is considered. We assume that there is a total of N subcarriers, and $L = N/K$ subcarriers are allocated to each user. The users are communicating with the base station through K statistically independent multipath wireless channels. In this paper, we consider the generalized subcarrier assignment scheme (G-CAS). In G-CAS, the base station

selects the best available subcarriers (i.e., the ones with the best SNRs) for each user, [3]. The $L \times 1$ vector $\mathbf{d}^{(i)}$ contains the data symbols of the i^{th} user. It is worth mentioning that the subcarriers of distinct users should be mapped onto mutually exclusive subsets of the available subcarriers. Hence, if the subcarriers allocated to the i^{th} and j^{th} users belong to the sets Ψ_i and Ψ_j, respectively, then $\Psi_i \cap \Psi_j = \emptyset, i \neq j$ and $\bigcup_{m=1}^{K} \Psi_m = \{1, \ldots, N\}$. In the OFDMA transmitter, the first step is subcarrier allocation. Thus, the i^{th} user signal vector after subcarrier mapping is

$$\mathbf{s}_{\mathrm{f}}^{(i)} = \mathbf{\Gamma}^{(i)} \mathbf{d}^{(i)}, \tag{1}$$

where the subscript f in $\mathbf{s}_{\mathrm{f}}^{(i)}$ stresses that the data is in the frequency domain and $\mathbf{\Gamma}^{(i)}$ is the $N \times L$ subcarrier allocation matrix of user i. $\mathbf{\Gamma}^{(i)}$ is comprised of the columns of an $N \times N$ identity matrix whose indices belong to the set Ψ_i. The output of the IDFT block for user i is given by

$$\mathbf{s}_{\mathrm{t}}^{(i)} = \mathbf{F}_N^{\mathrm{H}} \mathbf{s}_{\mathrm{f}}^{(i)}, \tag{2}$$

where $\mathbf{F}_N$ is the N-point DFT matrix with the elements $[\mathbf{F}_N]_{n,k} = \frac{1}{\sqrt{N}} e^{\frac{-j2\pi nk}{N}}$ for $n, k = 0, \ldots, N-1$. The subscript t in $\mathbf{s}_{\mathrm{t}}^{(i)}$ is to emphasise that the vector is in the time domain. Finally, the cyclic prefix (CP) and cyclic suffix (CS) whose lengths are N_{CP} and N_{CS}, will be appended to the first and last part of the signal[1]. In order to avoid self and multi-user interference due to the timing offsets of the users, a CP longer than both the maximum channel delay spread and the two way propagation delay is required. In addition, the cyclic extensions need to include some extra samples to be utilized for time domain windowing at the receiver which will be discussed in Section III. The residual timing errors will be incorporated in the channel impulse responses of the users; thereby, inter-symbol interference (ISI) between different users will be avoided [3]. The cyclically extended signal can be written as

$$\tilde{\mathbf{s}}_{\mathrm{t}}^{(i)} = \mathbf{T} \mathbf{s}_{\mathrm{t}}^{(i)}, \tag{3}$$

where $\mathbf{T} = [\mathbf{G}_{\mathrm{CP}}^{\mathrm{T}}, \mathbf{I}_N^{\mathrm{T}}, \mathbf{G}_{\mathrm{CS}}^{\mathrm{T}}]^{\mathrm{T}}$ is the corresponding cyclic extension matrix which is an $N_T \times N$ matrix. N_T is the length of an OFDMA symbol and $N_T = N + N_{\mathrm{CP}} + N_{\mathrm{CS}}$. The rows of $\mathbf{G}_{\mathrm{CP}}$ and $\mathbf{G}_{\mathrm{CS}}$ matrices include the last N_{CP} and the first N_{CS} rows of the identity matrix $\mathbf{I}_N$, respectively. The wireless channels for different users are assumed to be statistically independent with respect to each other and time invariant during one OFDMA symbol. If the channel impulse response for user i has the length equal to N_{ch} samples, it can be denoted by the vector $\mathbf{h}^{(i)} = [h_0^{(i)}, \ldots, h_{N_{\mathrm{ch}}-1}^{(i)}]^{\mathrm{T}}$ whose elements are assumed to be statistically independent complex Gaussian random variables. Considering the impact of CFOs from different users, the received signal is obtained as

$$\tilde{\mathbf{r}} = \sum_{i=1}^{K} \mathbf{\Phi}(\epsilon_i)(\mathbf{h}^{(i)} * \tilde{\mathbf{s}}_{\mathrm{t}}^{(i)}) + \boldsymbol{\nu}, \tag{4}$$

where $\mathbf{\Phi}(\epsilon_i)$ is the $N_{\mathrm{r}} \times N_{\mathrm{r}}$ diagonal CFO matrix whose diagonal elements are $\{1, e^{\frac{j2\pi\epsilon_i}{N}}, \ldots, e^{\frac{j2\pi\epsilon_i(N_{\mathrm{r}}-1)}{N}}\}$, $N_{\mathrm{r}} = N_T + N_{\mathrm{ch}} - 1$ and ϵ_i is the i^{th} user's CFO normalized by subcarrier spacing. Finally, $\boldsymbol{\nu}$ is the complex additive white Gaussian noise (AWGN) vector, i.e., $\boldsymbol{\nu} \sim CN(0, {\sigma_\nu}^2 \mathbf{I}_{N_{\mathrm{r}}})$ and ${\sigma_\nu}^2$ is the noise variance.

After discarding the cyclic extensions from $\tilde{\mathbf{r}}$, the result is passed through a DFT block. The output of the DFT block can be rearranged as, [11],

$$\bar{\mathbf{r}} = \mathbf{\Lambda} \mathbf{x} + \tilde{\boldsymbol{\nu}}. \tag{5}$$

Here, $\mathbf{\Lambda}$ is a CFO dependent $N \times N$ matrix that is called interference matrix. Also, $\mathbf{x}$ and $\tilde{\boldsymbol{\nu}}$ are, the composite data symbols of the users, affected by their respective channels, and the channel noise vector, respectively. A detailed definition of matrix $\mathbf{\Lambda}$ and vectors $\mathbf{x}$ and $\tilde{\boldsymbol{\nu}}$ is included in Section III. Direct solution of (5) is computationally demanding as it involves inversion of an $N \times N$ matrix, with N typically in the order of thousands. As noted earlier, many authors have proposed algorithms to reduce the complexity of solving (5), [11]–[15]. Nevertheless, these solutions are still computationally demanding. The goal of this paper is to revisit the same problem, but to propose a new class of algorithms leading to an order of magnitude or higher reduction in complexity.

III. Receiver Filtering for ICI Reduction

In conventional OFDMA receivers, after removing the cyclic extensions, DFT is applied to the received signal. This is equivalent to analyzing each received OFDM symbol through a bank of filters that are characterized by a rectangular prototype filter. Due to the fact that the rectangular filter has large side-lobes in its frequency response, such a filter bank system is prone to a significant amount of ICI when different subcarriers are not synchronized in frequency with respect to each other.

In order to reduce ICI to a limited number of adjacent subcarriers and hence, make the interference matrix quasi-banded[2], we borrow the following idea from the discrete multi-tone (DMT) literature[3]. To mitigate near-end cross-talk and radio frequency interference in very high bit-rate digital subscriber lines (VDSL), the authors of [21] proposed to replace the rectangular prototype filter/window in an OFDM receiver by a window with smooth roll-offs at the sides, e.g., see Fig. 1. A raised-cosine window is proposed for this application in [21]. Further study, in [23], indicates that the raised-cosine window is a good compromise choice. On the other hand, it is also noted in [21] that since the number of samples in the time domain are $N + N_{\mathrm{w}}$ and given that we need to analyze the signal samples in the frequency domain at N equally spaced samples, one may conveniently alias the time domain signal, as shown in Fig. 1, and then apply an N-point DFT to the result.

[1]Since, in OFDM systems, we are dealing with periodic signals, CS can be easily absorbed into CP and in that case a time shift of N_{CS} samples is needed. This time shift should be taken care of at the receiver and can be compensated at equalization stage.

[2]A quasi-banded matrix with bandwidth of $2D + 1$ is a matrix containing nonzero elements in the main diagonal, D bilateral diagonals around the main diagonal and D diagonals at the top-right and bottom-left corners of the matrix and the remaining elements are all zeros.

[3]DMT is the equivalent name for OFDM in the digital subscriber lines (DSL) literature.

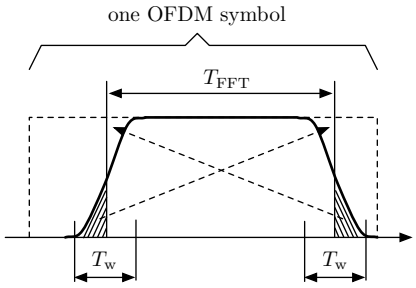

Fig. 1. A raised-cosine window and the process of aliasing in time domain. The excess samples beyond the length $T_{\rm FFT}$ on each side are added to the attenuated samples on the other side.

An analysis of the raised-cosine window that provides insight to its impact on side-lobe suppression is recently reported in [23]. It is noted that if $T_{\rm FFT}$ denotes the length of DFT and $T_{\rm w}$ the duration of the roll-off at each side, the raised-cosine window can be mathematically expressed as

$$g(t) = \text{rect}\left(\frac{t - T_{\rm FFT}/2}{T_{\rm FFT}}\right) * c(t), \tag{6}$$

where

$$c(t) = \frac{\pi}{2T_{\rm w}} \sin\left(\frac{\pi t}{T_{\rm w}}\right) \text{rect}\left(\frac{t - T_{\rm w}/2}{T_{\rm w}}\right), \tag{7}$$

and $\text{rect}(\cdot)$ is the rectangular function. Accordingly, in the frequency domain,

$$|G(f)| = T_{\rm FFT}|\text{sinc}(fT_{\rm FFT})| \times |C(f)|, \tag{8}$$

and

$$|C(f)| = \left|\frac{\cos(\pi f T_{\rm w})}{1 - 4f^2T_{\rm w}^2}\right|. \tag{9}$$

A point to note here is that $|C(f)|$ has a 'sinc' shape with the main lobe of $3/T_{\rm w}$ wide. It also drops to below -12 dB beyond the frequency range $(-1.1/T_{\rm w}, 1.1/T_{\rm w})$. If this attenuation is taken as sufficient to suppress the subcarrier side-lobes (numerical results presented later in Fig. 3 show this is a good compromise choice), one will find that the interference matrix becomes (with a good approximation) quasi-banded with a bandwidth of $2\lfloor 1.1T_{\rm FFT}/T_{\rm w}\rfloor + 1$, where $\lfloor\cdot\rfloor$ rounds down the number inside. It is worth nothing that beside the raised-cosine window, other window choices have been examined in [23] and the conclusion is that the raised cosine provides a good compromise choice. In the context of the work presented in this paper, we also conclude that the raised cosine window provides a good balance between the suppression of the out of band signals and the reduction of the bandwidth D. In our study, we made this conclusion by exploring the performance of our system when we used a trapezoidal window versus other window functions based on Hamming and Hanning functions.

As mentioned earlier, each OFDMA symbol has $N_{\rm CP}$ and $N_{\rm CS}$ cyclic extension samples at the beginning and the end, respectively. Since, the first $N_{\rm GI}$ samples of $\tilde{\mathbf{r}}$ in (4) are affected by the channels of the users, in order to avoid ISI and also leave enough samples for the receiver windowing process, the lengths of the CP and CS need to be $N_{\rm GI}+\frac{N_{\rm w}}{2}$ and $\frac{N_{\rm w}}{2}$, respectively. Discarding the first $N_{\rm GI}$ samples using guard interval removal matrix $\mathbf{R}_{\rm GI} = [\mathbf{0}_{(N+N_{\rm w})\times N_{\rm GI}}, \mathbf{I}_{(N+N_{\rm w})}]$, we have

$$\mathbf{r} = \sum_{i=1}^{K} e^{\frac{j2\pi\epsilon_i N_{\rm GI}}{N}} \widetilde{\mathbf{\Phi}}(\epsilon_i)\bar{\mathbf{T}}\mathbf{H}_{\rm t}^{(i)}\mathbf{s}_{\rm t}^{(i)} + \mathbf{R}_{\rm GI}\boldsymbol{\nu}, \tag{10}$$

where $\widetilde{\mathbf{\Phi}}(\epsilon_i) = \text{diag}(1, e^{\frac{j2\pi\epsilon_i}{N}}, \ldots, e^{\frac{j2\pi\epsilon_i(N+N_{\rm w}-1)}{N}})$, $\bar{\mathbf{T}} = [\mathbf{G}_{\rm W}^{\rm T}, \mathbf{I}_N^{\rm T}, \mathbf{G}_{\rm CS}^{\rm T}]^{\rm T}$. The sub-matrices $\mathbf{G}_{\rm W}$ and $\mathbf{G}_{\rm CS}$ are of the size $\frac{N_{\rm w}}{2}\times N$ and consist of the last and the first $\frac{N_{\rm w}}{2}$ rows of the identity matrix $\mathbf{I}_N$, respectively. $\mathbf{H}_{\rm t}^{(i)}$ is the $N\times N$ circulant channel matrix of user i with the first column $\mathbf{h}^{(i)}$ being zero padded to have the length of N. The windowed and aliased signal can be presented as

$$\mathbf{r}' = \sum_{i=1}^{K} e^{\frac{j2\pi\epsilon_i N_{\rm GI}}{N}} (\bar{\mathbf{T}}^{\rm T}\mathbf{W}\widetilde{\mathbf{\Phi}}(\epsilon_i)\bar{\mathbf{T}})\mathbf{H}_{\rm t}^{(i)}\mathbf{s}_{\rm t}^{(i)} + \bar{\mathbf{T}}^{\rm T}\mathbf{W}\mathbf{R}_{\rm GI}\boldsymbol{\nu}, \tag{11}$$

where $\mathbf{W} = \text{diag}(\mathbf{w}_{\rm rc})$, $\mathbf{w}_{\rm rc}$ is the raised-cosine window vector and $\bar{\mathbf{T}}^{\rm T}$ does the aliasing operation as mentioned earlier. Since, $\mathbf{H}_{\rm t}^{(i)}$ is a circulant matrix, it can be spectrally factorized as $\mathbf{F}_N^{\rm H}\mathbf{H}_{\rm f}^{(i)}\mathbf{F}_N$ where $\mathbf{H}_{\rm f}^{(i)}$ is the $N\times N$ diagonal matrix whose diagonal elements are the channel frequency response of the user i. Hence, recalling (2), $\mathbf{H}_{\rm t}^{(i)}\mathbf{s}_{\rm t}^{(i)}$ can be written as $\mathbf{F}_N^{\rm H}\mathbf{H}_{\rm f}^{(i)}\mathbf{s}_{\rm f}^{(i)}$ and after passing the signal through the DFT block, we have

$$\begin{aligned}\bar{\mathbf{r}} &= \mathbf{F}_N\mathbf{r}' \\ &= \sum_{i=1}^{K} e^{\frac{j2\pi\epsilon_i N_{\rm GI}}{N}} (\mathbf{F}_N\bar{\mathbf{T}}^{\rm T}\mathbf{W}\widetilde{\mathbf{\Phi}}(\epsilon_i)\bar{\mathbf{T}}\mathbf{F}_N^{\rm H})\mathbf{H}_{\rm f}^{(i)}\mathbf{s}_{\rm f}^{(i)} + \tilde{\boldsymbol{\nu}} \\ &= \mathbf{\Lambda}\mathbf{x} + \tilde{\boldsymbol{\nu}},\end{aligned} \tag{12}$$

where

$$\mathbf{x} = \sum_{i=1}^{K} e^{\frac{j2\pi\epsilon_i N_{\rm GI}}{N}} \mathbf{H}_{\rm f}^{(i)}\mathbf{s}_{\rm f}^{(i)} = \bar{\mathbf{H}}_{\rm f}\bar{\mathbf{d}}, \tag{13}$$

and

$$\mathbf{\Lambda} = \sum_{i=1}^{K} \mathbf{F}_N\bar{\mathbf{T}}^{\rm T}\mathbf{W}\widetilde{\mathbf{\Phi}}(\epsilon_i)\bar{\mathbf{T}}\mathbf{F}_N^{\rm H}\mathbf{\Pi}^{(i)}, \tag{14}$$

is the $N\times N$ interference matrix, $\mathbf{\Pi}^{(i)} = \mathbf{\Gamma}^{(i)}(\mathbf{\Gamma}^{(i)})^{\rm H}$ and $\tilde{\boldsymbol{\nu}} = \mathbf{F}_N\bar{\mathbf{T}}^{\rm T}\mathbf{W}\mathbf{R}_{\rm GI}\boldsymbol{\nu}$. $\bar{\mathbf{H}}_{\rm f}$ is an $N\times N$ diagonal matrix which contains the composite channel frequency responses of all the users in its diagonal elements. It is worth mentioning that the phase factors $e^{\frac{j2\pi\epsilon_i N_{\rm GI}}{N}}$ are absorbed into the composite channel of the users. The composite data vector $\bar{\mathbf{d}}$ includes the information symbols of all the users corresponding to their allocated subcarriers as if there has been no interference.

As noted before, windowing at the receiver confines the interference generated by each subcarrier only to a number of its neighbouring subcarriers which depends on the roll-off factor of the window. Fig. 2, shows a snapshot of the interference power from each subcarrier to the others for both cases of OFDMA system with and without receiver windowing. In Fig. 2, we consider an OFDMA system with 32 subcarriers, 4 users and $\text{CFOs} = [0.20, -0.35, 0.45, -0.11]$ where G-CAS is deployed. From Fig. 2, one may notice that the interference power from each subcarrier to the others in the system with receiver filtering is very small after a certain

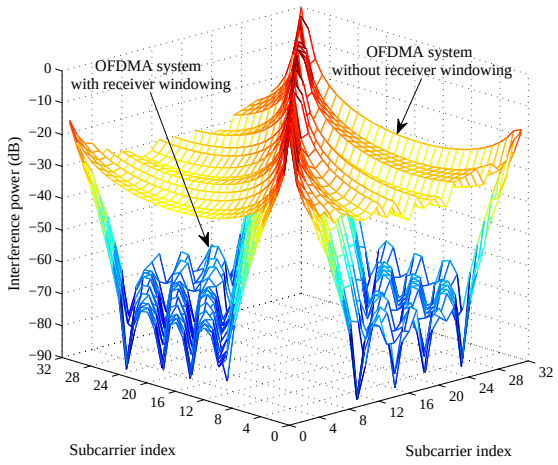

Fig. 2. Interference power between different subcarriers for G-CAS case when $N = 32,\ K = 4,\ N_{\rm w} = 8,\ \text{CFOs} = [0.20, -0.35, 0.45, -0.11]$ for the systems with and without receiver filtering.

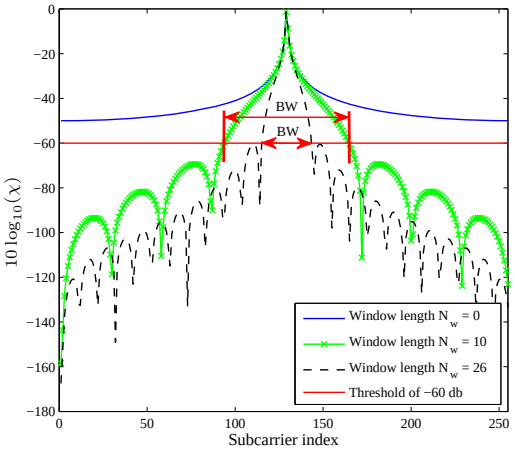

Fig. 3. Interference power for different values of $N_{\rm w}$ and the threshold line of -60 dB for an uplink scenario where $N = 256$ and $\epsilon_{\max} = 0.4$.

modulo-N distance and hence may be considered as negligible. Thus, the interference matrix can be approximated with a quasi-banded matrix with very good precision. The simulation results which will be presented in Section VII will attest to this fact. In contrast, in a system without receiver windowing, the interference power from each subcarrier to the other ones is large. Therefore, approximation of the interference matrix with a banded one as is proposed in [11] will result in a significant performance loss especially in presence of users with large CFOs, [14].

Accordingly, we can write the interference matrix as the summation of a quasi-banded matrix, $\mathbf{\Lambda}_{\rm QB}$, and the matrix $\mathbf{\Lambda}_{\rm I}$ which contains the negligible elements of $\mathbf{\Lambda}$ outside the certain bandwidth of $2D+1$.

$$[\mathbf{\Lambda}_{\rm QB}]_{m,n} = \begin{cases} [\mathbf{\Lambda}]_{m,n}, & |m-n| \le D, \\ & \text{and } |m-n| \ge N-D, \\ 0, & \text{otherwise}, \end{cases} \qquad (15)$$

where the bandwidth of the matrix $\mathbf{\Lambda}_{\rm QB}$ is $2D+1$. Also, $\mathbf{\Lambda}_{\rm I} = \mathbf{\Lambda} - \mathbf{\Lambda}_{\rm QB}$.

Discussion

The parameter D needs to be designed in a way to consider the dominant interference terms of the matrix $\mathbf{\Lambda}$. To that end, the maximum CFO, $\epsilon_{\max} = \max\ |\epsilon_i|$ for $i = 0, \ldots, K-1$, should be considered and the interference terms due to $\epsilon_{\max}$ need to be generated. The interference terms can be obtained by taking N-point DFT from the main diagonal of the matrix

$$\mathbf{\Xi} = \bar{\mathbf{T}}^{\rm T}\mathbf{W}\widetilde{\mathbf{\Phi}}(\epsilon_{\max})\bar{\mathbf{T}}, \qquad (16)$$

where $\widetilde{\mathbf{\Phi}}(\epsilon_{\max}) = \text{diag}(1, e^{\frac{j2\pi\epsilon_{\max}}{N}}, \ldots, e^{\frac{j2\pi\epsilon_{\max}(N+N_{\rm w}-1)}{N}})$, $\mathbf{\Xi} = \text{diag}(\boldsymbol{\xi})$ and $\boldsymbol{\xi}$ contains the windowed and aliased version of the vector $[1, e^{\frac{j2\pi\epsilon_{\max}}{N}}, \ldots, e^{\frac{j2\pi\epsilon_{\max}(N+N_{\rm w}-1)}{N}}]^{\rm T}$. Thus, the interference terms can be found as $\boldsymbol{\chi} = \mathbf{F}_N\boldsymbol{\xi}$. The interference terms in the vector $\boldsymbol{\chi}$ with power less than -60 dB may be neglected and replaced by zero. Accordingly, the number of non-zero elements that remain is equal to $2D+1$. Thereby, the parameter D can be designed.

As a case in point, Fig. 3 illustrates the interference terms for different values of $N_{\rm w}$ and the threshold line of -60 dB for an uplink scenario where $N = 256$ and $\epsilon_{\max} = 0.4$. As mentioned above, the interference terms below this threshold are negligible and can be replaced by zero. Additionally, Fig. 3 depicts the localization of interference power with respect to different values of $N_{\rm w}$. As can be seen, the system without receiver windowing suffers from a large amount of interference and none of the interference terms falls below -60 dB. In contrast, for the system with receiver windowing and $N_{\rm w} = 10$ a large number of interference terms fall below -60 dB and as $N_{\rm w}$ increases to 26 the interference power becomes more localized. As a result, a larger number of interference terms can be neglected and the bandwidth of the interference matrix is further reduced. Therefore, the parameter D for $N_{\rm w} = 10$ and $N_{\rm w} = 26$ can be designed as $D = 34$ and $D = 12$, respectively.

IV. ZF-based CFO Compensation

Since, the interference matrix is full rank (see Appendix A, for a proof); given the received signal model in (12), the ICI caused by multiple CFOs can be completely removed based on the ZF criterion [11], viz.,

$$\hat{\mathbf{x}}_{\rm ZF} = \mathbf{\Lambda}^{-1}\bar{\mathbf{r}} = \mathbf{x} + \mathbf{\Lambda}^{-1}\tilde{\boldsymbol{\nu}}. \qquad (17)$$

However, in practice, where N may be many hundreds, or even thousands, the computational complexity of the matrix inversion in (17) may be prohibitively high. Examples are in WiMAX IEEE 802.16e and 3GPP LTE standards, where N can be as large as 2048 [24], [25].

As noted in Section III, due to the effect of receiver filtering, the interference matrix $\mathbf{\Lambda}$ can be approximated with the quasi-banded matrix $\mathbf{\Lambda}_{\rm QB}$. This, as shown in the rest of this paper, allows us to implement the ZF and MMSE solutions with an affordable complexity.

ZF solution is expressed as

$$\hat{\mathbf{x}}_{\rm ZF} = \mathbf{\Lambda}_{\rm QB}^{-1}\bar{\mathbf{r}} = \mathbf{x} + \mathbf{\Lambda}_{\rm QB}^{-1}\mathbf{\Lambda}_{\rm I}\mathbf{x} + \mathbf{\Lambda}_{\rm QB}^{-1}\tilde{\boldsymbol{\nu}}. \qquad (18)$$

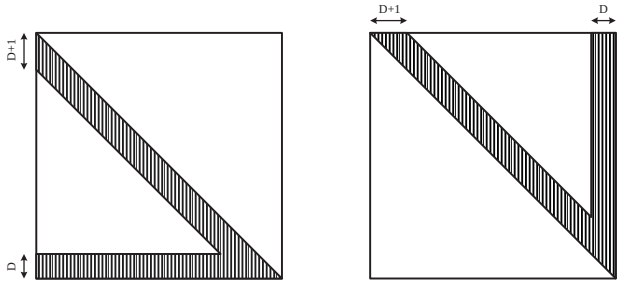

Fig. 4. (a) and (b) depict the structure of $\mathbf{L}$ and $\mathbf{U}$ matrices after LU factorization of a quasi-banded matrix, respectively.

Clearly, the approximation of $\mathbf{\Lambda}$ by the banded matrix $\mathbf{\Lambda}_{\rm QB}$ results in some residual interference; $\mathbf{\Lambda}_{\rm QB}^{-1}\mathbf{\Lambda}_{\rm I}\mathbf{x}$ on the right-hand side of (18). However, as will be shown in Section VII, this residual interference is so negligible that does not have any impact on the bit error rate (BER) performance of the system.

Due to the fact that receiver filtering does not bring a great amount of reduction to the subcarrier sidelobes that are close to the main lobe, [23], after receiver filtering, even for small CFO ranges the system with G-CAS suffers from a great amount of self-user interference and MAI which need to be canceled. To this end, in the following subsections, we propose three CFO compensation techniques based on the ZF criterion. All of our proposed techniques have low computational complexity, thanks to the banded property of $\mathbf{\Lambda}_{\rm QB}$. Unlike solutions proposed in [13] and [12], our proposed techniques here are not limited to a particular subcarrier assignment. They all are applicable to G-CAS.

A. LU Factorization

Due to the banded form of the matrix $\mathbf{\Lambda}_{\rm QB}$, it can be efficiently factorized into a pair of lower and upper triangular matrices ($\mathbf{\Lambda}_{\rm QB} = \mathbf{LU}$). In general, LU factorization of a quasi-banded matrix leads to a pair of upper and lower triangular matrices with a V-shape structure, similar to the one in Fig. 4. However, in the case of interest in this paper, since the off-diagonal elements of $\mathbf{\Lambda}_{\rm QB}$ are all less than one in amplitude and are decreasing very fast as they move away from the main diagonal, one will find that the elements of $\mathbf{L}$ and $\mathbf{U}$ matrices vanish as they move away from the corners. Fig. 5 highlights this fact for a typical example of the lower triangular matrix. Likewise, the upper triangular matrix follows the same structure as that of the matrix $\mathbf{L}^{\rm T}$. Hence, $\mathbf{L}$ and $\mathbf{U}$ can be approximated with upper and lower quasi-banded matrices. As a result, the LU factorization can be implemented with a low computational complexity.

Once the LU factorization is performed, the vector $\mathbf{x}$ is calculated, simply, by using the forward and backward substitution method [22]. The large number of zero elements in the lower and upper triangular matrices significantly reduces the complexity of forward and backward substitutions. The numerical results in Section VII prove the high accuracy of this approximation when compared with the case where the full interference matrix is considered.

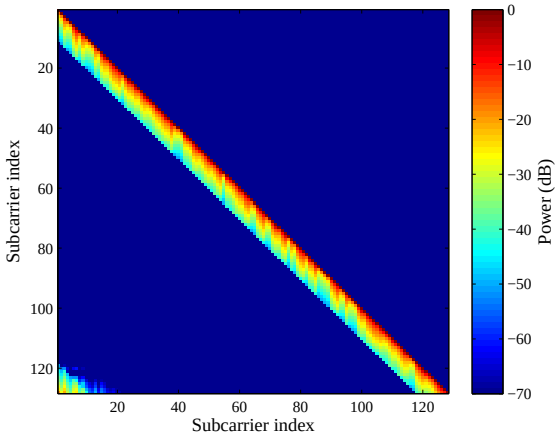

Fig. 5. The matrix $\mathbf{L}$ for G-CAS case when $N = 128,\ K = 4,\ \text{CFOs} = [0.27, -0.35, -0.43, 0.12]$.

B. Truncated Neumann Series

The matrix $\mathbf{\Lambda}_{\rm QB}^{-1}$ can be approximated using truncated von Neumann series to reduce the computational cost of the ZF solution even more than that of the LU factorization method. $\mathbf{\Lambda}_{\rm QB}$ can be written as the summation of its diagonal, $\mathbf{D}$, and its off-diagonal part, $\tilde{\mathbf{\Lambda}}$, and rearrange the result as

$$\begin{aligned}\mathbf{\Lambda}_{\rm QB} &= \mathbf{D} + \tilde{\mathbf{\Lambda}} \\ &= \mathbf{D}(\mathbf{I}_N + \mathbf{D}^{-1}\tilde{\mathbf{\Lambda}}).\end{aligned} \tag{19}$$

Next, we note that ${\mathbf{\Lambda}_{\rm QB}}^{-1} = (\mathbf{I}_N + \mathbf{D}^{-1}\tilde{\mathbf{\Lambda}})^{-1}\mathbf{D}^{-1}$ and $(\mathbf{I}_N + \mathbf{D}^{-1}\tilde{\mathbf{\Lambda}})^{-1}$ can be approximated using the $M^{\rm th}$ order truncation of the Neumann series

$$(\mathbf{I}_N + \mathbf{D}^{-1}\tilde{\mathbf{\Lambda}})^{-1} = \sum_{i=0}^{M}(-\mathbf{D}^{-1}\tilde{\mathbf{\Lambda}})^i, \tag{20}$$

if the spectral radius[4] of the matrix $\mathbf{D}^{-1}\tilde{\mathbf{\Lambda}}$ is smaller than one. A smaller spectral radius allows adoption of a smaller value of M, and hence a further reduction of complexity in the implementation of (20).

Since, in G-CAS case, the interference matrix does not follow any particular structure, it is difficult (if not impossible) to mathematically identify the spectral radius of $\mathbf{D}^{-1}\tilde{\mathbf{\Lambda}}$. Here, we resort to a numerical analysis and find the probability density function (PDF) of the spectral radius of $\mathbf{D}^{-1}\tilde{\mathbf{\Lambda}}$ as CFOs take random values. Fig. 6 presents sample examples of such PDF for the cases where $N = 512, 1024$, $K = 4, 32$, and CFOs are chosen randomly from the interval of $[-0.25, 0.25]$. The PDFs are obtained based on 1,000,000 random choices of CFOs. For all the cases, the spectral radius of $\mathbf{D}^{-1}\tilde{\mathbf{\Lambda}}$ is limited by some upper bound that is less than one. In order to study the effect of the increase in the number of users we have considered the case where $N = 512, K = 32$ and compared it with the case where $N = 512, K = 4$. As it can be observed from Fig. 6, for the same number of subcarriers, as the number of users increases, the spectral radius becomes more concentrated to values around 0.4 with a

[4]Spectral radius of a square matrix $\mathbf{A}$ refers to the amplitude of its largest eigenvalue.

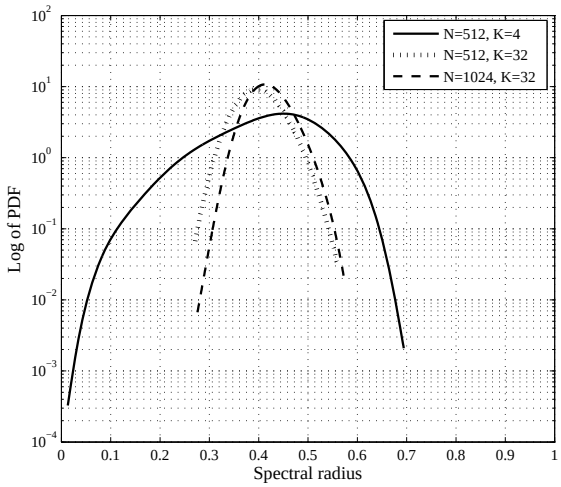

Fig. 6. Spectral radius of the matrix $\mathbf{D}^{-1}\tilde{\mathbf{\Lambda}}$ for a system with the CFOs in the range of $[-0.25, 0.25]$.

higher probability. From comparison of the PDF of the cases where $N = 512, K = 32$ and $N = 1024, K = 32$, one can conclude that increasing the number of subcarriers does not have a dramatic effect on the lower and upper bound of the spectral radius of $\mathbf{D}^{-1}\tilde{\mathbf{\Lambda}}$. Additional tests reveal that the spectral radius of $\mathbf{D}^{-1}\tilde{\mathbf{\Lambda}}$ gets smaller as the range of CFOs reduces, and it gets larger as the range increases. For the broader ranges beyond $[-0.25, 0.25]$, the spectral radius of $\mathbf{D}^{-1}\tilde{\mathbf{\Lambda}}$ approaches one and in that case M has to be increased and this in turn increases the complexity. Moreover, as CFOs spread over a wider range, beyond $[-0.4, 0.4]$, the spectral radius of $\mathbf{D}^{-1}\tilde{\mathbf{\Lambda}}$ may exceed one and in that case the Neumann series diverges. Hence, the method described here will not be applicable.

Taking note of the above observations, we propose to use the Neumann series expansion for the case where CFOs fall in a range of $[-0.25, 0.25]$ or smaller, and switch to other methods (e.g., the LU-factorization) when CFOs spread over a wider range. At the same time, it should be noted that the range $[-0.25, 0.25]$ is relatively relaxed and can be easily retained in practice. See [16] where the authors have argued that the range $[-0.2, 0.2]$ is a very relaxed one. They have noted that the aforementioned CFO range is much larger than the 2% maximum CFO requirement of IEEE 802.16a standard.

Using (19) and (20) in (18), we obtain

$$\hat{\mathbf{x}}_{\mathrm{ZF}}^{(M)} = \left(\sum_{i=0}^{M} (-\mathbf{D}^{-1}\tilde{\mathbf{\Lambda}})^i \right) \mathbf{D}^{-1}\bar{\mathbf{r}}. \tag{21}$$

To keep the complexity of implementation of this equation at a minimum level, it may be implemented recursively according to the algorithm listed in the following table (Algorithm 1). Each step of the algorithm involves a matrix by vector multiplication (multiplication of $-\mathbf{D}^{-1}\tilde{\mathbf{\Lambda}}$ by $\hat{\mathbf{x}}_{\mathrm{ZF}}^{(i-1)}$) followed by a vector addition (addition of $\hat{\mathbf{x}}_{\mathrm{ZF}}^{(0)}$). Moreover, noting that $-\mathbf{D}^{-1}\tilde{\mathbf{\Lambda}}$ is a very sparse matrix (most of its elements are zero), the complexity of the multiplication $(-\mathbf{D}^{-1}\tilde{\mathbf{\Lambda}})\hat{\mathbf{x}}_{\mathrm{ZF}}^{(i-1)}$ remains relatively small; see Section VI for details.

Algorithm 1 Interference cancellation algorithm based on truncated Neumann series

1: $\hat{\mathbf{x}}_{\mathrm{ZF}}^{(0)} = \mathbf{D}^{-1}\bar{\mathbf{r}}$ ▷ initialization
2: **for** $i = 1$ to M **do**
3: $\quad \hat{\mathbf{x}}_{\mathrm{ZF}}^{(i)} = (-\mathbf{D}^{-1}\tilde{\mathbf{\Lambda}})\hat{\mathbf{x}}_{\mathrm{ZF}}^{(i-1)} + \hat{\mathbf{x}}_{\mathrm{ZF}}^{(0)}$
4: **end for**

C. Conjugate Gradient Algorithm

The CG algorithm is only applicable to the linear systems of equations with positive definite and Hermitian coefficient matrices [26]. Therefore, in order to be able to estimate the transmitted symbols of different users based on the ZF criterion using the CG algorithm, both sides of (12) can be multiplied by $\mathbf{\Lambda}^{\mathrm{H}}$. Therefore, the ZF solution in (17) can be reformulated as $\hat{\mathbf{x}}_{\mathrm{ZF}} = (\mathbf{\Lambda}^{\mathrm{H}}\mathbf{\Lambda})^{-1}\mathbf{\Lambda}^{\mathrm{H}}\bar{\mathbf{r}}$. From approximation of $\mathbf{\Lambda}$ with $\mathbf{\Lambda}_{\mathrm{QB}}$, equation (18) can be rearranged as

$$\hat{\mathbf{x}}_{\mathrm{ZF}} = \mathbf{P}_{\mathrm{ZF}}^{-1}\mathbf{\Lambda}^{\mathrm{H}}\bar{\mathbf{r}}, \tag{22}$$

where $\mathbf{P}_{\mathrm{ZF}} = \mathbf{\Lambda}^{\mathrm{H}}\mathbf{\Lambda}$. The Hermitian and positive definite property of $\mathbf{P}_{\mathrm{ZF}}$ allows utilization of the CG algorithm for another low complexity computation of $\hat{\mathbf{x}}_{\mathrm{ZF}}$. This idea was first suggested in [14], where authors used the special structure of the interference matrix $\mathbf{\Lambda}$ to propose a low complexity MMSE solution. Although the same solution (with some minor modifications) is applicable to the case of interest to this paper as well, here, the banded nature of $\mathbf{\Lambda}_{\mathrm{QB}}$ and $\mathbf{P}_{\mathrm{ZF}}$ allows a more direct and lower complexity implementation of the CG algorithm. The pseudo code that is presented under Algorithm 2 lists the CG algorithm when applied for computation of $\hat{\mathbf{x}}_{\mathrm{ZF}}$, [26]. The subscript/superscript i indicates the iteration index, δ is the convergence tolerance and $\hat{\mathbf{x}}_{\mathrm{CG}}^{(i)}$ is the estimation of $\hat{\mathbf{x}}_{\mathrm{ZF}}$ at the i^{th} iteration of the CG algorithm. Finally, the vectors $\mathbf{d}_i$ and $\boldsymbol{\xi}_i$ denote the search direction and residual vectors in the i^{th} iteration, respectively. The complexity of this algorithm is dominated by matrix to vector multiplication $\mathbf{P}_{\mathrm{ZF}}\mathbf{d}_i$. In [14], the special form of $\mathbf{\Lambda}$ is taken advantage of and $\mathbf{P}_{\mathrm{ZF}}\mathbf{d}_i$ is implemented using a sequence of FFT/IFFT operations. Here, we note that since $\mathbf{P}_{\mathrm{ZF}}$ is banded (sparse), direct calculation of $\mathbf{P}_{\mathrm{ZF}}\mathbf{d}_i$ results in a lower complexity.

The CG algorithm has to run over a number of iterations to converge. The number of iterations depends on the eigenvalue spread of the underlying matrix, $\mathbf{P}_{\mathrm{ZF}}$. In [14] it is noted that the eigenvalue spread of $\mathbf{P}_{\mathrm{ZF}}$ is rather limited and hence the authors have concluded that the CG algorithm will converge within a number of iterations that is much smaller than N. The same conclusion is applicable to our proposed implementation.

V. MMSE-based CFO Compensation

Even though the ZF solution removes the effect of the CFOs, multiplication of $\mathbf{\Lambda}_{\mathrm{QB}}^{-1}$ to the noise in (18) may result in noise enhancement. In order to avoid the noise enhancement problem, it is common to use MMSE criterion. This leads to a balance between residual self/multiple user interference and noise enhancement at the detector output. The MMSE solution

Algorithm 2 The CG algorithm

$\boldsymbol{\xi}_0 = \mathbf{P}_{\rm ZF}\hat{\mathbf{x}}_{\rm CG}^{(0)} - \boldsymbol{\Lambda}_{\rm QB}^{\rm H}\bar{\mathbf{r}}$
$\mathbf{d}_1 = \boldsymbol{\xi}_0$
$i = 0$
while $\|\boldsymbol{\xi}_i\| \geq \delta \|\boldsymbol{\xi}_0\|$ **do**
  $i = i + 1$
  $\alpha_i = \frac{\boldsymbol{\xi}_{i-1}^{\rm H}\boldsymbol{\xi}_{i-1}}{\mathbf{d}_i^{\rm H}\mathbf{P}_{\rm ZF}\mathbf{d}_i}$
  $\hat{\mathbf{x}}_{\rm CG}^{(i)} = \hat{\mathbf{x}}_{\rm CG}^{(i-1)} + \alpha_i\mathbf{d}_i$
  $\boldsymbol{\xi}_i = \boldsymbol{\xi}_{i-1} + \alpha_i\mathbf{P}_{\rm ZF}\mathbf{d}_i$
  $\gamma_i = \frac{\boldsymbol{\xi}_i^{\rm H}\boldsymbol{\xi}_i}{\boldsymbol{\xi}_{i-1}^{\rm H}\boldsymbol{\xi}_{i-1}}$
  $\mathbf{d}_{i+1} = \mathbf{d}_i + \gamma_i\mathbf{d}_i$
end while

of (12) with quasi-banded approximation of the interference matrix is given by

$$\hat{\mathbf{x}}_{\rm MMSE} = \mathbf{P}^{-1}\boldsymbol{\Lambda}_{\rm QB}^{\rm H}\bar{\mathbf{r}}, \tag{23}$$

where $\mathbf{P} = \boldsymbol{\Lambda}_{\rm QB}^{\rm H}\boldsymbol{\Lambda}_{\rm QB} + {\sigma_\nu}^2\mathbf{I}_N$, [11]. We refer to (23) as MMSE CFO compensator.

Similar to its ZF counterpart, the MMSE CFO compensator can also benefit from the quasi-banded property of the interference matrix which enables the development of a class of low complexity algorithms. In particular, the matrix $\mathbf{P}$ is also banded, however, it has a bandwidth that can be as much as twice the bandwidth of $\boldsymbol{\Lambda}_{\rm QB}$. Hence, the MMSE CFO compensator algorithms that are presented below, expectedly, have a higher complexity than the ZF CFO compensator algorithms that were presented in the previous section.

A. LU Factorization

In the same fashion as in Section IV-A, the matrix $\mathbf{P}$ can be efficiently factorized into lower and upper triangular matrices and $\hat{\mathbf{x}}_{\rm MMSE}$ can be estimated using forward and backward substitutions technique. Clearly, the wider bandwidth of $\mathbf{P}$, compared to that of $\boldsymbol{\Lambda}_{\rm QB}$, leads to a higher complexity. Complexity details are given in the next section.

B. Truncated Neumann Series

The same as in Section IV-B, we can write $\mathbf{P}$ as the sum of its main diagonal and off-diagonal elements. Therefore, $\mathbf{P}^{-1}$ can be rearranged as $(\mathbf{I}_N + \mathbf{D}_P^{-1}\tilde{\mathbf{P}})^{-1}\mathbf{D}_P^{-1}$ where $\mathbf{D}_P$ and $\tilde{\mathbf{P}}$ contain the diagonal and off-diagonal elements of $\mathbf{P}$, respectively. If the spectral radius of $\mathbf{D}_P^{-1}\tilde{\mathbf{P}}$ is smaller than one, a similar iterative algorithm to the one presented in Algorithm 1, based on $M^{\rm th}$ order truncation of Neumann series can be developed to estimate $\hat{\mathbf{x}}_{\rm MMSE}$. Thus, we have

$$\hat{\mathbf{x}}_{\rm MMSE}^{(M)} = \left(\sum_{i=0}^{M}(-{\mathbf{D}_P}^{-1}\tilde{\mathbf{P}})^i\right){\mathbf{D}_P}^{-1}\boldsymbol{\Lambda}_{\rm QB}^{\rm H}\bar{\mathbf{r}}. \tag{24}$$

Fig. 7 depicts PDF of the spectral radius of $\mathbf{D}_P^{-1}\tilde{\mathbf{P}}$ for the cases of having $N = 512, 1024$ subcarriers and $K = 4, 32$ users where the CFOs are in the range of $[-0.25, 0.25]$. The PDFs are derived based on $1,000,000$ random choices of CFOs for the G-CAS case. About the effects of the number of subcarriers and users on the spectral radius of $\mathbf{D}_P^{-1}\tilde{\mathbf{P}}$, we have similar observations as in Section IV-B. Based on Fig. 7, in all the cases, the upper bound for the spectral radius of $\mathbf{D}_P^{-1}\tilde{\mathbf{P}}$ is approximately 0.9 which guarantees convergence of the Neumann series. For the same reasons as in Section IV-B, we propose this solution for the cases where CFOs fall in the range of $[-0.25, 0.25]$.

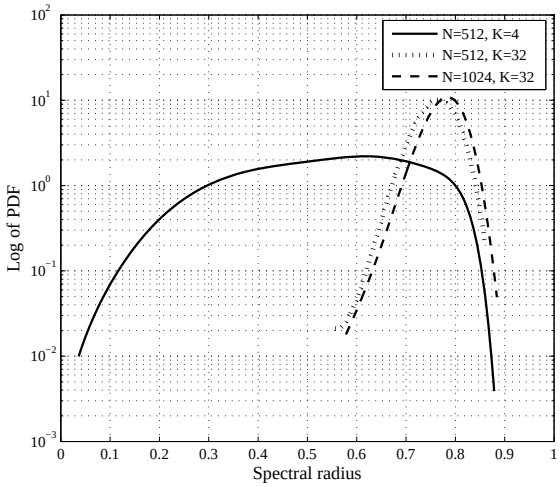

Fig. 7. Spectral radius of the matrix $\mathbf{D}_P^{-1}\tilde{\mathbf{P}}$ for a system with the CFOs in the range of $[-0.25, 0.25]$.

Comparing Fig. 6 and Fig. 7, one may realize that the spectral radius of the matrix $\mathbf{D}_P^{-1}\tilde{\mathbf{P}}$ in MMSE case is larger than the spectral radius of the matrix $\mathbf{D}^{-1}\tilde{\boldsymbol{\Lambda}}$ in ZF case, for the same CFO range. Thus, our MMSE solution based on Neumann series needs more iterations to converge than its ZF counterpart which translates into a higher complexity.

C. Conjugate Gradient Algorithm

As the only difference between $\mathbf{P}$ and $\mathbf{P}_{\rm ZF}$ is their main diagonal, following the same line of derivations as in Section IV-C, the MMSE estimates of the transmitted signals can be found simply by replacing $\mathbf{P}_{\rm ZF}$ with $\mathbf{P}$ in Algorithm 2.

VI. Computational Complexity

Table I summarizes the computational complexity of the ZF and MMSE CFO compensation techniques/algorithms that were developed in the previous sections and compares them with the direct solutions[5] and the CG algorithm of [14]. The reader should be reminded that prior to this work, the CG algorithm of [14] was the technique with lowest complexity applicable to G-CAS. We thus use this as a base to evaluate the effectiveness of the methods developed in this paper.

Following our earlier notations, the total number of subcarriers and the number of users are denoted by N and K, respectively. The parameters I, D and $N_{\rm w}$ in the table indicate the number of iterations, bandwidth of the interference matrix $\boldsymbol{\Lambda}_{\rm QB}$ and roll-off width of the receiver window, respectively. All the operations involve complex numbers. Therefore, we provide the computational complexity expressions based on

[5]Direct solutions include direct inversion and multiplication of the matrices involved to the received signal, $\bar{\mathbf{r}}$.

TABLE I
COMPUTATIONAL COMPLEXITY OF DIFFERENT CFO COMPENSATION TECHNIQUES

Technique	Number of CMs for ZF-based CFO compensation	Number of CMs for MMSE-based CFO compensation
Direct	$\frac{1}{3}N^3+2N^2+\frac{KN}{2}\log_2 N$	$\frac{5}{6}N^3+\frac{5}{2}N^2+\frac{KN}{2}\log_2 N$
Proposed LU factorization	$\frac{1}{3}D^3+(2N-1)D^2+(4N-\frac{1}{3})D+\frac{KN}{4}\log_2 N+N_{\rm w}$	$\frac{9}{8}D^3+\frac{9}{4}(\frac{17}{6}N-1)D^2+(\frac{43}{4}N-\frac{1}{2})D+2N+\frac{KN}{4}\log_2 N+N_{\rm w}$
Proposed Truncated series	$I(2ND+N)+N+\frac{KN}{4}\log_2 N+N_{\rm w}$	$I(3ND+N)+\frac{15}{8}ND^2+\frac{19}{4}ND+3N+\frac{KN}{4}\log_2 N+N_{\rm w}$
Proposed CG	$I(4ND+7N)+N(2D+1)+\frac{KN}{4}\log_2 N+N_{\rm w}$	$I(4ND+7N)+N(2D+1)+\frac{KN}{4}\log_2 N+N_{\rm w}$
CG, [14]	$I(KN\log_2 N+2KN+5N)+KN\log_2 N+2KN$	$I(KN\log_2 N+2KN+5N)+KN\log_2 N+2KN$

the number of complex multiplications (CMs). Direct ZF and MMSE solutions involve direct inversion of the matrices $\mathbf{\Lambda}$ and $\mathbf{P}$, respectively. Since, we approximate $\mathbf{\Lambda}$ with $\mathbf{\Lambda}_{\rm QB}$ in our proposed algorithms, there is no need to calculate all the elements of $\mathbf{\Lambda}$. Accordingly, FFT pruning techniques can be utilized to further reduce the computational cost of calculating $\mathbf{\Lambda}_{\rm QB}^{-1}$, [27], following the CG algorithm of [14].

All the proposed solutions in this paper include time domain windowing that needs $N_{\rm w}$ CMs. In order to calculate the columns of the matrix $\mathbf{\Lambda}_{\rm QB}$, as only $2D+1$ elements out of N are needed, FFT pruning techniques can be utilized and hence $\frac{KN}{4}\log_2 N$ CMs need to be performed. In ZF-based LU factorization solution, the number of complex multiplications that are needed for calculation of the lower and upper triangular matrices as well as forward and backward substitutions is equal to $\frac{1}{3}D^3+(2N-1)D^2+(4N-\frac{1}{3})D$. In MMSE-based LU factorization, the complexity overhead with respect to the ZF-based solution is mainly laid in multiplication of $\mathbf{\Lambda}_{\rm QB}^{\rm H}$ to $\bar{\mathbf{r}}$ and calculation of $\mathbf{\Lambda}_{\rm QB}^{\rm H}\mathbf{\Lambda}_{\rm QB}$. This complexity overhead is $\frac{19}{24}D^3+\frac{5}{4}(3.5N-1)D^2+(\frac{27}{4}N-\frac{1}{6})D+2N$. The ZF technique based on the truncated Neumann series needs N CMs for initialization step and $2ND+N$ CMs per iteration. In the same way as for the MMSE-based LU factorization technique, there exists a complexity overhead with respect to the ZF-based solution which is equal to $\frac{15}{8}ND^2+\frac{19}{4}ND+2N$ CMs and ND complex multiplications per iteration. As can be understood from Table I, both CG-based ZF and MMSE techniques that we propose have the same computational complexity which is due to the equations that were discussed in Sections IV and V. Multiplication of $\mathbf{\Lambda}_{\rm QB}^{\rm H}$ to $\bar{\mathbf{r}}$ involves $N(2D+1)$ CMs. In addition, $4ND+7N$ number of CMs is needed for each iteration.

The computational cost for CFO compensation in single user systems is low and thus affordable from a practical implementation point of view. It involves N complex multiplications and an N-point FFT operation. In order to provide a good understanding of the level of complexity of the various CFO compensation techniques, we normalize the complexity of all of them to that of a single user receiver and present the results. This allows us to assess the practicality of different solutions.

The complexity formulas presented in Table I are evaluated for the case where $N=2048$ and the results after normalization with respect to that of a single user receiver are presented in Fig. 8. Different numbers of iterations are required for convergence of different algorithms. Hence, we consider $I=2$ and 4 for our proposed Neumann series based ZF and MMSE techniques, respectively and $I=32$ for the CG-based algorithms (as is prescribed in [14]). The parameters, roll-off width of the receiver window and bandwidth of the interference matrix are set as $N_{\rm w}=\lfloor 0.1N \rfloor$ and $D=10$, respectively. These results reveal the following instructive and interesting facts:

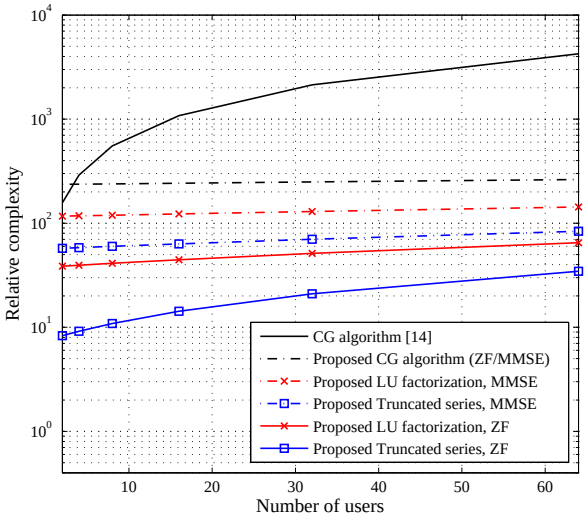

Fig. 8. Relative complexity of different CFO compensation techniques with respect to single user case when N = 2048.

- The complexity of CG algorithm of [14] is at least over two orders of magnitude larger than that of a single user receiver. It even grows to over three orders of magnitude as the number of users increases. Although the processing is done at the base station, these complexity numbers are clearly excessively large.
- The ZF solution based on the Neumann series brings down the complexity by two orders of magnitude, hence, leads to a much more affordable implementation.
- Other algorithms/solutions that are proposed in this paper also have complexities that are lower than the complexity of the CG algorithm.

On the other hand, the simulation results that are presented in the next section reveal that the performance difference between the ZF and MMSE solutions is negligible. Hence, given the low complexity advantage of the ZF solutions based on LU factorization and Neumann series, there is no reason to adopt an MMSE solution for CFO compensation. For cases where CFOs remain in the range of $\pm 25\%$ of carrier spacing, the ZF solution based on the Neumann series which has the lowest complexity and provides the optimal performance should be adopted. For a higher CFO range than $\pm 25\%$ of carrier spacing, LU factorization method should be utilized.

VII. Numerical Results

In this section, we present the bit error rate (BER) performance of our proposed solutions in the uplink of an OFDMA system for different cases. We assume different numbers of subcarriers and users with generalized carrier allocation scheme. The multipath channel SUI-2 proposed by the IEEE802.16 broadband wireless access working group, [28], is considered. The CP is chosen long enough to accommodate both the wireless channel delay spread and the samples needed for the receiver windowing operation, i.e., $N_{\rm CP} = 0.25N$. The users with uncoded 4-QAM and 16-QAM modulation schemes are considered in our numerical evaluations and each point in the results is based on $10,000$ simulation runs. In each simulation run, random subcarrier indices based on G-CAS are allocated to the users. The CFOs, ϵ_i's, are independently chosen from a uniform distribution. In this section, different CFO ranges of $\pm 25\%$ and $\pm 50\%$ of subcarrier spacing are considered[6]. A raised-cosine window with the roll-off width of $N_{\rm w} = \lfloor 0.1N \rfloor$ samples is used. The bandwidth $D = 10$ is chosen for the quasi-banded approximation of the interference matrix.

The performance of the proposed ZF solutions are investigated and compared with that of the direct solution[7] for the CFO range of $\pm 25\%$ subcarrier spacing for two cases: in Fig. 9, we consider $N = 512,\ K = 4$ and 4-QAM; whereas in Fig. 10, we use $N = 1024,\ K = 32$ and 16-QAM modulation. We investigate the BER performance of our algorithms for small and large number of users with two constellation sizes to show the efficacy of our proposed algorithms. As Figs. 9 and 10 depict, in both cases, the LU factorization technique has a BER performance similar to the direct solution with a negligible performance loss at very high signal-to-noise ratios (SNRs). This shows that approximation of $\mathbf{L}$ and $\mathbf{U}$ matrices as quasi-banded ones, as predicted, is accurate enough to guarantee a satisfactory performance. However, the second order truncation of Neumann series incurs a performance loss of around 1 dB and 3 to 4 dB at high SNRs for the cases of Fig. 9 and Fig. 10, respectively. This performance loss at high SNRs can be avoided by adding one more iteration to the Neumann series. This of course constitutes a small increase in complexity.

As noted in Section IV-B, for large CFOs up to 50% subcarrier spacing, convergence of the Neumann series, unfortunately, is not guaranteed and thus, such method cannot be used. Fig. 11, illustrates the performance of our proposed ZF-based LU factorization and CG techniques and compares them with those of the direct ZF solution and the MMSE-based CG algorithm of [14] for $\epsilon_i \in [-0.5, 0.5),\ N = 512,\ K = 4$ and 4-QAM modulation. In Fig. 12, we have investigated the performance of our proposed ZF-based techniques and compared them with that of the direct solution for the case of having a larger number of users and subcarriers; namely:

[6]In all cases, normalized CFOs with respect to subcarrier spacing are considered and therefore our results are valid for any arbitrary subcarrier spacing.

[7]Direct solution involves direct inversion and multiplication of the matrix $\mathbf{\Lambda}$ to the received signal, $\bar{\mathbf{r}}$.

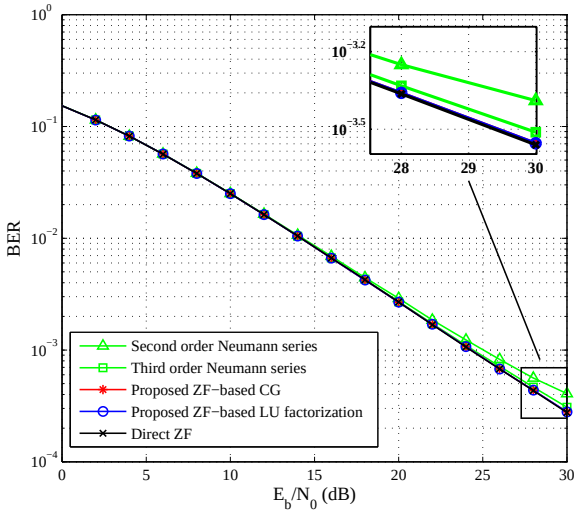

Fig. 9. BER performance of our proposed techniques compared with the direct ZF solution for the uplink of OFDMA systems with G-CAS, 4-QAM, $N = 512$ and $K = 4$ when $|\epsilon_i| \leq 0.25$.

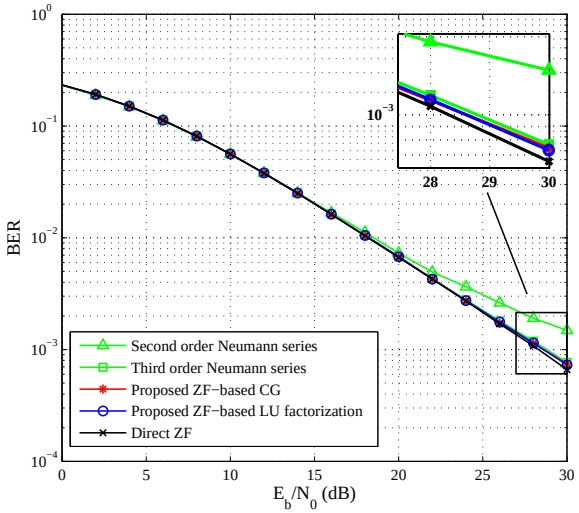

Fig. 10. BER performance of our proposed techniques compared with the direct ZF solution for the uplink of OFDMA systems with G-CAS, 16-QAM, $N = 1024$ and $K = 32$ when $|\epsilon_i| \leq 0.25$.

$K = 32$ and $N = 1024$ and larger constellation size of 16-QAM. Figs. 11 and 12 indicate the robust performance of our proposed ZF-based LU factorization and CG techniques under harsh CFO conditions. In [14], Lee et al. have shown that their MMSE-based solution provides the optimal performance. Comparing the performance of the proposed MMSE solution in [14] with our LU factorization technique reveals that in this particular application, MMSE and ZF solutions provide very close BER curves (Fig. 11). As emphasized in Section VI, the proposed ZF solutions have a lower computational complexity compared with that of the MMSE solutions. Accordingly, the ZF techniques are more practical and hence attractive for the uplink of OFDMA systems. As highlighted in Section VI, our ZF solution based on truncated Neumann series which is applicable to the CFO range of $\pm 25\%$ has the lowest complexity. Therefore, only when CFOs may be out of the

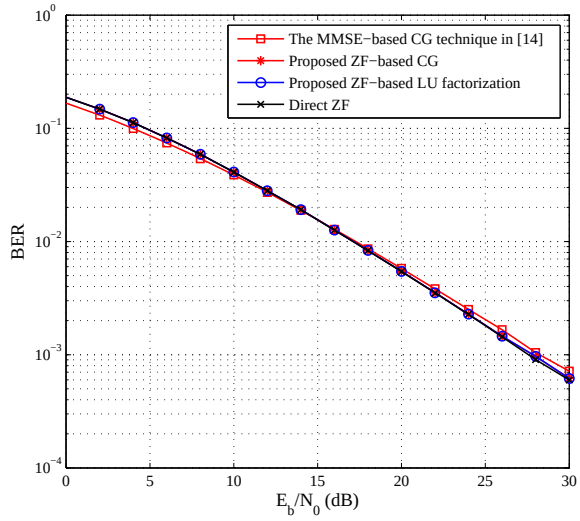

Fig. 11. BER performance of our proposed techniques compared with the direct ZF solution and the solution in [14] for the uplink of OFDMA systems with G-CAS, 4-QAM, $N = 512$ and $K = 4$ when $|\epsilon_i| < 0.5$.

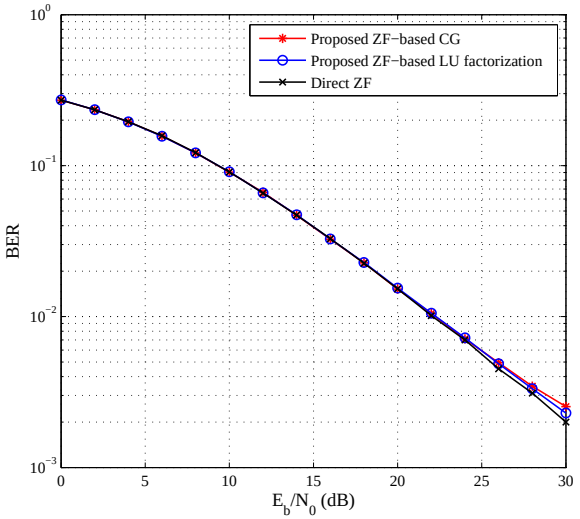

Fig. 12. BER performance of our proposed techniques compared with the direct ZF solution for the uplink of OFDMA systems with G-CAS, 16-QAM, $N = 1024$ and $K = 32$ when $|\epsilon_i| < 0.5$.

range $\pm 25\%$ other solutions should be considered and in that case the clear choice (considering the computational complexity) is ZF-based LU factorization.

A point to note, here, is that the same CP length is considered for all the techniques that are compared in this section. However, for some solutions like direct ZF and that of [14] where no receiver filtering is required, a shorter CP is sufficient. Consequently, their CP can be $N_{\rm w} = \lfloor 0.1N \rfloor$ samples shorter than the one required for our proposed solutions. Therefore, our proposed solutions in this paper lead to around 1 dB BER performance loss compared with the direct ZF or the solution proposed in [14].

VIII. Conclusion

In this paper, we developed a new class of low complexity receivers for the uplink of orthogonal frequency division multiple access (OFDMA) systems through utilization of receiver windowing techniques. All the algorithms that have been developed in this paper are applicable to the generalized subcarrier allocation scheme (G-CAS). Time domain receiver windowing enables reduction of the interference induced by multiple carrier frequency offsets (CFOs). This leads to a class of low complexity CFO compensation techniques that can reduce the computational complexity of the receiver up to over two orders of magnitude, when compared to the lowest complexity algorithm in the literature. This great reduction in complexity comes at the expense of a longer cyclic extension, i.e., a compromise in bandwidth efficiency. Both zero forcing (ZF) and minimum mean squared error (MMSE) compensators were thoroughly studied and for each, a number of solutions were developed. Simulations showed that all solutions lead to the same bit error rate performance and thus the choice between different CFO compensation algorithms is dictated by their computational complexity. While the proposed ZF-based Neumann series compensator was found to be the simplest, it works only when the CFO range is limited to approximately $\pm 25\%$ of carrier spacing. For cases where CFOs fall outside of the range of $\pm 25\%$ of carrier spacing, the proposed ZF-based LU factorization method should be adopted. The complexity analysis presented in this paper was in the unit of single user complexity. The research presented in this paper led to CFO compensation algorithms whose complexity was only one order of magnitude greater than that of the single user case while keeping very close to the optimal performance. Such a substantial complexity reduction makes our algorithms feasible in practice and therefore, suitable for hardware implementation of real-time uplink OFDMA systems.

Appendix A
Proof of Full Rank Property of Λ

Using (14), the interference matrix $\mathbf{\Lambda}$ can be written as

$$\begin{aligned}\mathbf{\Lambda} &= \mathbf{F}_N \bar{\mathbf{T}}^{\rm T} \mathbf{W} \sum_{i=1}^{K} \widetilde{\mathbf{\Phi}}(\epsilon_i) \bar{\mathbf{T}} \mathbf{F}_N^{\rm H} \mathbf{\Pi}^{(i)} \\ &= \mathbf{F}_N \bar{\mathbf{T}}^{\rm T} \mathbf{W} \mathbf{\Omega}, \end{aligned} \tag{A.1}$$

where

$$\mathbf{\Omega} = \sum_{i=1}^{K} \widetilde{\mathbf{\Phi}}(\epsilon_i) \bar{\mathbf{T}} \mathbf{F}_N^{\rm H} \mathbf{\Pi}^{(i)} = [\boldsymbol{\omega}_0, \ldots, \boldsymbol{\omega}_{N-1}], \tag{A.2}$$

and $\boldsymbol{\omega}_\ell$s are the column vectors of the matrix $\mathbf{\Omega}$.

Since the DFT matrix, $\mathbf{F}_N$, is full rank, if we show that all the rows of $\bar{\mathbf{T}}^{\rm T} \mathbf{W} \mathbf{\Omega}$ are linearly independent, we can conclude that the interference matrix is also full rank. The matrix $\mathbf{\Omega}$ is an $(N + N_{\rm w}) \times N$ matrix with the $\ell^{\rm th}$ column of

$$\begin{aligned}\boldsymbol{\omega}_\ell &= \big[e^{-\frac{j2\pi}{N}(\frac{N_{\rm w}}{2})(\epsilon_j+\ell)}, \ldots, e^{-\frac{j2\pi}{N}(\epsilon_j+\ell)}, \\ &\quad 1, e^{\frac{j2\pi}{N}(\epsilon_j+\ell)}, \ldots, e^{\frac{j2\pi}{N}(N-1)(\epsilon_j+\ell)}, \\ &\quad e^{j2\pi(\epsilon_j+\ell)}, \ldots, e^{\frac{j2\pi}{N}(N+\frac{N_{\rm w}}{2}-1)(\epsilon_j+\ell)}\big]^{\rm T} \times \\ &\quad e^{\frac{j2\pi N_{\rm w}}{2N}\epsilon_j}, \end{aligned} \tag{A.3}$$

where $\ell \in \Psi_j$. From (A.3), one may notice that the elements of the vector in the right hand side are all different powers of

$e^{\frac{j2\pi}{N}(\epsilon_j+\ell)}$ scaled by $e^{\frac{j2\pi N_{\rm w}}{2N}\epsilon_j}$. Hence, in order to make the columns of the matrix $\mathbf{\Omega}$ linearly dependent, there should be two columns ℓ and ℓ' that satisfy the following condition

$$\ell + \epsilon_j = \ell' + \epsilon_k, \tag{A.4}$$

where $\ell \in \Psi_j$ and $\ell' \in \Psi_k$. Therefore, $|\ell - \ell'| = |\epsilon_k - \epsilon_j|$. Due to the fact that ℓ and ℓ' are column indices, they are different integers and $|\ell - \ell'|$ is also an integer while ϵ_k and ϵ_j are residual CFOs in the range of $(-0.5, 0.5]$. Thereby, $|\epsilon_k - \epsilon_j| < 1$ and (A.4) does not hold. Thus, we can conclude that all the columns in $\mathbf{\Omega}$ are linearly independent and therefore the rank of $\mathbf{\Omega}$ is N. The general rule for finding the rank of the product of matrices $\mathbf{A}$ and $\mathbf{B}$ is as follows [22]

$$\mathrm{Rank}(\mathbf{AB}) = \mathrm{Rank}(\mathbf{B}) - \mathrm{Dim}\big(\mathrm{Null}(\mathbf{A}) \cap \mathrm{Range}(\mathbf{B})\big), \tag{A.5}$$

where $\mathbf{A}$ and $\mathbf{B}$ are $n \times p$ and $p \times q$ matrices, respectively. Since $\mathrm{Rank}(\mathbf{\Omega}) = N$ and there is no intersection between the nullspace of $\mathbf{W}$ and the range of $\mathbf{\Omega}$, $\mathrm{Dim}\big(\mathrm{Null}(\mathbf{W}) \cap \mathrm{Range}(\mathbf{\Omega})\big) = 0$, the matrix $\mathbf{W\Omega}$ has also rank of N. Similarly, $\mathrm{Null}(\bar{\mathbf{T}}^{\rm T}) \cap \mathrm{Range}(\mathbf{W\Omega}) = \emptyset$ and the matrix $\bar{\mathbf{T}}^{\rm T}\mathbf{W\Omega}$ is full rank.

ACKNOWLEDGMENT

This work is supported by Science Foundation of Ireland through the CTVR and CONNECT grants 10/CE/i1853 and 13/RC/2077, respectively.

REFERENCES

[1] A. Farhang, A. Javaid Majid, N. Marchetti, L. E. Doyle, and B. Farhang-Boroujeny, "Interference localization for uplink OFDMA systems in presence of CFOs," *Proc. of the IEEE WCNC 2014*, April 2014.

[2] K. Raghunath and A. Chockalingam, "SIR analysis and interference cancellation in uplink OFDMA with large carrier frequency/timing offsets," *IEEE Trans. Wireless Commun.*, vol. 8, no.5, pp. 2202–2208, May 2009.

[3] M. Morelli, C. C. J. Kuo, and M. O. Pun, "Synchronization techniques for orthogonal frequency division multiple access (OFDMA): A tutorial review," *Proc. of the IEEE*, vol. 95, no.7, pp. 1394–1427, July 2007.

[4] Y. Na and H. Minn, "Line search based iterative joint estimation of channels and frequency offsets for uplink OFDM systems," *IEEE Trans. Wireless Commun.*, vol. 6, no. 12, pp. 4374–4382, 2007.

[5] X. N. Zeng and A. Ghrayeb, "Joint CFO and channel estimation for OFDMA uplink: an application of the variable projection method," *IEEE Trans. Wireless Commun.*, vol. 8, no. 5, pp. 2306–2311, 2009.

[6] S. Yerramalli, M. Stojanovic, and U. Mitra, "Carrier Frequency Offset Estimation for Uplink OFDMA Using Partial FFT Demodulation," in *IEEE Global Telecommunications Conference, GLOBECOM*, 2010.

[7] K. Lee, S.-H. Moon, and I. Lee, "Low-complexity leakage-based carrier frequency offset estimation techniques for OFDMA uplink systems," in *IEEE Global Telecommunications Conference, GLOBECOM*, 2010.

[8] ——, "A pilot-aided frequency offset estimation algorithm for OFDMA uplink systems," in *IEEE Vehicular Technology Conference (VTC Fall)*,, 2012.

[9] T. Yucek and H. Arslan, "Carrier frequency offset compensation with successive cancellation in Uplink OFDMA Systems," *IEEE Trans. Wireless Commun.*, vol. 6, no.10, pp. 3546–3551, Oct. 2007.

[10] S. Ahmed and L. Zhang, "Low complexity iterative detection for OFDMA uplink with frequency offsets," *IEEE Trans. Wireless Commun.*, vol. 8, no. 3, pp. 1199–1205, 2009.

[11] Z. Cao, U. Tureli, and Y.-D. Yao, "Low-complexity orthogonal spectral signal construction for generalized OFDMA uplink with frequency synchronization errors," *IEEE Trans. Veh. Technol.*, vol. 56, no. 3, pp. 1143–1154, May 2007.

[12] A. Farhang, N. Marchetti, and L. Doyle, "Low Complexity LS and MMSE Based CFO Compensation Techniques for the Uplink of OFDMA Systems," *Proc. of the IEEE ICC '13*, June 2013.

[13] C. Y. Hsu and W. R. Wu, "A low-complexity zero-forcing CFO compensation scheme for OFDMA uplink systems," *IEEE Trans. Wireless Commun.*, vol. 7, no.10, pp. 3657–3661, Oct. 2008.

[14] K. Lee, S.-R. Lee, S.-H. Moon, and I. Lee, "MMSE-based CFO compensation for uplink OFDMA systems with conjugate gradient," *IEEE Trans. Wireless Commun.*, vol. 11, no.8, pp. 2767–2775, Aug. 2012.

[15] K. Lee and I. Lee, "CFO compensation for uplink OFDMA systems with conjugated gradient," *Proc. of the IEEE ICC '11*, pp. 1–5, June 2011.

[16] H. Defeng and K. B. Letaief, "An interference-cancellation scheme for carrier frequency offsets correction in OFDMA systems," *IEEE Trans. Commun.*, vol. 53, no.7, pp. 1155–1165, July 2005.

[17] G. Chen, Y. Zhu, and K. B. Letaief, "Combined MMSE-FDE and interference cancellation for uplink SC-FDMA with carrier frequency offsets," *Proc. of the IEEE ICC '10*, pp. 1–5, May 2010.

[18] P. Schniter, "Low-complexity equalization of OFDM in doubly selective channels," *IEEE Trans. Signal Processing.*, vol. 52, no. 4, pp. 1002–1011, 2004.

[19] M. Huang, X. Chen, S. Zhou, and J. Wang, "Iterative ICI cancellation algorithm for uplink OFDMA system with carrier-frequency offset," *IEEE 62nd Vehicular Technology Conference,*, vol. 3, pp. 1613–1617, Fall 2005.

[20] D. Boswarthick, O. Hersent, and O. Elloumi, *M2M communications : a systems approach*. Wiley-Blackwell, 2012.

[21] F. Sjoberg, R. Nilsson, M. Isaksson, P. Odling, and P. Borjesson, "Asynchronous Zipper," *Proc. of the IEEE ICC '99*, pp. 231–235 vol.1, 1999.

[22] C. D. Meyer, *Matrix Analysis and Applied Linear Algebra*. SIAM, 2001.

[23] B. Farhang-Boroujeny, "OFDM Versus Filter Bank Multicarrier," *Signal Processing Magazine, IEEE*, vol. 28, no. 3, pp. 92–112, 2011.

[24] "IEEE standard for local and metropolitan area networks, part 16: air interface for fixed and mobile broadband wireless access systems amendment 2: physical and medium access control layers for combined fixed and mobile operation in licensed bands and corrigendum 1," *IEEE 802.16e-2005*, Feb. 2006.

[25] "3GPP TS 36.211, Evolved Universal Terrestrial Radio Access (E-UTRA); Physical channels and modulation," *3GPP*, 2011.

[26] G. H. Golub and C. F. Van Loan, *Matrix computations (3rd Ed.)*. Johns Hopkins University Press, 1996.

[27] J. Markel, "FFT pruning," *IEEE Trans. Audio and Electroacoustics*, vol. 19, no. 4, pp. 305–311, 1971.

[28] The IEEE802.16 Broadband Wireless Access Working Group, Channel Models for Fixed Wireless Applications [Online]. Available: http://www.ieee802.org/16/tg3/contrib/802163c-01_29r4.pdf.

Arman Farhang received his BSc. in telecommunications engineering from Azad University of Najafabad, Iran in 2007. He received MSc. in telecommunications engineering from Sadjad University of Technology, Mashhad, Iran in 2010. Currently, he is pursuing a Ph.D. degree in Irish National Telecommunications Research Centre (CTVR/CONNECT) at Trinity College Dublin, Ireland. His research interests include wireless communications, digital signal processing for communications, multiuser communications and multicarrier systems.

Nicola Marchetti is currently Assistant Professor at Trinity College Dublin, Ireland, where he holds the Ussher Lectureship in Wireless Communications, and is a member of the Irish National Telecommunications Research Centre (CTVR/CONNECT). He received the Ph.D. in Wireless Communications from Aalborg University, Denmark in 2007, and the M.Sc. in Electronic Engineering from University of Ferrara, Italy in 2003. He also holds a M.Sc. in Mathematics which he received from Aalborg University in 2010. He worked as a Research Assistant at the University of Ferrara in 2003-2004. He then was a Ph.D. Student in 2004-2007, and a Research and Teaching Post-Doc in 2007-2010 at Aalborg University. His former collaborations include research projects in cooperation with Samsung, Nokia Siemens Networks, Huawei, Intel Mobile Communications among others. His research interests include: 5G Wireless Communication Systems, Cognitive Radio and Dynamic Spectrum Access, Complex Systems Science, Integrated Optical-Wireless Networks, Multiple Antenna Systems, Radio Resource Management, Small Cells and HetNets, and Waveforms. He authored 60 refereed journals and conference papers, hold 2 patents, and wrote 2 books and 4 book chapters.

Linda E. Doyle is Professor of Engineering and The Arts in Trinity College, University of Dublin. She is the Director of CTVR/CONNECT, an SFI Research centre focused on future networks and communications. CTVR/CONNECT is headquartered in Trinity College, comprises ten academic institutions in total and has over 40 industry partners. Prof. Doyle's expertise is in the fields of wireless communications, cognitive radio, reconfigurable networks, spectrum management and creative arts practices.

She has published widely in these domains and leads a large research team within CTVR/CONNECT. Prof. Doyle a member of the Ofcom Spectrum Advisory Board in the UK. She is a Fellow Of Trinity College Dublin.

Behrouz Farhang-Boroujeny (M84-SM90) received the B.Sc. degree in electrical engineering from Teheran University, Iran, in 1976, the M.Eng. degree from University of Wales Institute of Science and Technology, UK, in 1977, and the Ph.D. degree from Imperial College, University of London, UK, in 1981. From 1981 to 1989 he was with the Isfahan University of Technology, Isfahan, Iran. From 1989 to 2000 he was with the National University of Singapore. Since August 2000, he has been with the University of Utah.

He is an expert in the general area of signal processing. His current scientific interests are adaptive filters, multicarrier communications, detection techniques for space-time coded systems, and cognitive radio. In the past, he has worked and has made significant contribution to areas of adaptive filters theory, acoustic echo cancellation, magnetic/optical recoding, and digital subscriber line technologies. He is the author of the books "Adaptive Filters: theory and applications", John Wiley & Sons, 1998, and "Signal Processing Techniques for Software Radios", self published at Lulu publishing house, 2009 and 2010 (second edition).

Dr. Farhang-Boroujeny received the UNESCO Regional Office of Science and Technology for South and Central Asia Young Scientists Award in 1987. He served as an associate editor of IEEE Trans. on Signal Processing from July 2002 to July 2005, and as an associate editor of IEEE Signal Processing Letters from April 2008 to March 2010. He has also been involved in various IEEE activities, including the chairmanship of the Signal Processing/Communications chapter of IEEE of Utah in 2004 and 2005.